Journal of Applied Polymer Science

# Poly(2,6-di(thiophene-2-yl)-3,5bis(4-(thiophene-2-yl)phenyl)dithieno [3,2-b;2′,3′-d]thiophene)/Carbon Nanotube Composite for Capacitor Applications

**Murat Ates,[1] Nuri Eren,[1] Ipek Osken,[2] Suzan Baslilar,[2] Turan Ozturk[2,3]**

[1]Department of Chemistry, Faculty of Arts and Sciences, Namik Kemal University, Degirmenalti Campus, 59030 Tekirdag, Turkey
[2]Department of Chemistry, Faculty of Arts and Sciences, Istanbul Technical University, Maslak, Istanbul, Turkey
[3]Chemistry Group, Organic Chemistry Laboratory, TUBITAK UME, PBox 54, 41470, Gebze-Kocaeli, Turkey
Correspondence to: M. Ates (E-mail: mates@nku.edu.tr) or T.Ozturk (E-mail: ozturktur@itu.edu.tr)

**ABSTRACT:** A novel monomer, 2,6-di(thiophene-2-yl)-3,5bis(4-(thiophene-2-yl)phenyl)dithieno[3,2-*b*;2',3'-*d*]thiophene ($Th_4DTT$) has been synthesized and used as an electro-active material. It has been electropolymerized onto glassy carbon (GC) electrode in sodium dodecyl sulfate (SDS) solution (0.1 M) together with multi-walled carbon nanotubes (MWCNT). A good capacitive characteristics for P($Th_4DTT$)/MWCNT composite has been obtained by electrochemical impedance spectroscopy (EIS), which is, to our best knowledge, the first report on capacitor behavior of a dithienothiophene. A synergistic effect has been resolved by Nyquist, Bode-magnitude—phase and admittance plots. Specific capacitance of the conducting polymer/MWCNT, calculated from cyclic voltammogram (CV) together with area and charge formulas, has been found to be 20.17 F $g^{-1}$. Long-term stability of the capacitor has also been tested by CV, and the results indicated that, after 500 cycles, the specific capacitance is 87.37% of the initial capacitance. An equivalent circuit model of $R_s(C_1(R_1(Q(R_2W))))(C_2R_3)$ has been obtained to fit the experimental and theoretical data. The double layer capacitance ($C_{dl}$) value of P($Th_4DTT$)/MWCNT (4.43 mF $cm^{-2}$) has been found to be 25 times higher than P($Th_4DTT$) ($C_{dl}$= 0.18 mF $cm^{-2}$). © 2013 Wiley Periodicals, Inc. J. Appl. Polym. Sci. **2014**, *131*, 40061.

**KEYWORDS:** synthesis and processing; nanotubes; graphene and fullerenes; functionalization of polymers; conducting polymers; coatings

Received 5 August 2013; accepted 14 October 2013
**DOI: 10.1002/app.40061**

## INTRODUCTION

As the energy is one of the most important topics for human being, development of renewable and clean energy sources has been continuing to be among the top hot research subjects and will be in near future. High-performance batteries and capacitors take important part in these subjects,[1] among which, electrochemical supercapacitors (ECs) have a special importance due to their advantages like high capacitive storage, fast charge/discharge performance and long cycle-life.[2] Two types of ECs, based on charge storage mechanisms are available. Electric double-layer (EDL) capacitors generally use carbon-based active materials, having high surface areas as electrodes, and energy storage is performed through separation of electronic and ionic charges at electrode-electrolyte interface. The second type of ECs is known as pseudo-capacitors or redox supercapacitors. Their performance is based on charge storage through fast and reversible surface or near-surface Faradic reactions[3,4] of redox active electrode materials, such as metal oxides and conducting polymers.[5,6]

Considerable attention has been focused on redox electrochemical capacitors, containing conducting polymers, which enhance highly the stored energy through Faradic processes. Thin film polymer electrodes are widely used in such energy storage devices, which have three possible configurations, i.e., supercapacitors, having (i) two electrodes constituted by the same *p*-dopable conducting polymer, (ii) two different *p*-dopable conducting polymers, and (iii) a *p*- and *n*-dopable conducting polymer, among which configuration (iii) is the most favored one due to its energy and power densities. However, complex morphology of the conducting polymers plays an important role in their physical properties. Generally, their conjugation length, interchain interactions and extent of disorder are significant parameters, governing the final characteristics of the resulting polymers.[7,8]

Design, syntheses, and preparation of conducting polymer films has been an increasingly important subject of intensive research,[9,10] owing to the fact that these films can possess desirable physical, chemical, and electrochemical properties for many applications, such as supercapacitors, energy storage batteries, electronic,[11,12] optoelectronic,[13,14] chemo-sensor,[15,16] photochromic,[17] and nonlinear optical devices.[18,19] The concept of improving mechanical, thermal, electrical or physical properties of materials through addition of reinforcements has received a great momentum after the seminal work on carbon nanotube (CNT) by Iijima in 1991.[20] CNT has exceptionally high elastic modulus (stiffness) and tensile strength (strengths), which is 10–100 times higher than the strongest steel as a fraction of weight.[21] It displays unique electrical properties and has 1000 time higher electric current carrying capacity than copper.[22] The properties of CNT are a kind of mixture of diamond (strong and thermally conductive) and graphite (electrically conductive) as well as light and very flexible,[23] which make CNT prime candidate for the development of potentially new composite materials with improved mechanical properties and electrical conductivity. CNT–polymer composites have a variety of prospective applications ranging from ultra strong materials for bullet proof vests, high performance materials for space and aeronautics, biosensor, super capacitor for electrode applications in modern electronics.[24,25]

A rapid progress has already been made in the development of hybrid materials, incorporating conducting polymers and carbon nanotubes (CNT), which is a promising route to attain synergistic effect[26–28] and find applications in the fabrication of various electronic devices, ranging from super capacitors to biochips.[29–31] Carbon nanotubes possess inherent extraordinary structural, mechanical, electrical, electronic and thermal behaviors.[32,33] In the past few years, CNT/conducting polymer composites have been used for many promising technological applications such as corrosion resistance, battery, solar cell, sensor, energy storage, microelectronics, and optoelectronic devices.[34–41] Conducting polymers such as poly(3,4-ethylenedioxythiophene) (PEDOT)/CNT for generating a hole-conducting layer in organic light-emitting diodes[42] and poly(3-octylthiophene)/CNT[43] and poly(*p*-phenylene venylene) (PPV)/(CNT)[44] for highly efficient photovoltaic cells[45] have been studied. Furthermore, it was reported that multi-walled carbon nanotubes (MWCNTs) can store nearly twice energy density per mass unit than single-walled carbon nanotubes (SWCNTs).[46,47] Because of the better accessibility of the ions to the electrochemically active surface, which is responsible for higher values of capacitance, nanometer-sized and well-ordered mesoporous structures should be suitable for further increasing the capacitance performance of conducting polymers. Swelling and shrinkage of PANI caused by a volume change during the insertion/removal of counter ions must be considered since the mechanical stress in polymer film.

In this work, a novel dithienothiophene derivative, 2,6-di(thiophene-2-yl)−3,5bis(4-(thiophene-2-yl)phenyl)dithieno[3,2-*b*;2',3'-*d*] thiophene ($Th_4DTT$) was synthesized and characterized by $^1H$ NMR, $^{13}C$ NMR, and FT-IR, which was then electropolymerized on a glassy carbon electrode with dispersed MWCNTs in 0.1 M SDS. Modified thin film was characterized by FTIR, SEM-EDX, and EIS analyses. This study presents a new circuit model parameters obtained from $R_s(C_1(R_1(Q(R_2W))))(C_2R_3)$.

## EXPERIMENTAL

### Materials

The 3,4-ethylenedioxythiophene (EDOT), tetraethylammonium tetrafluoroborate (99%), dimethyl formamide (DMF), tetrahydrofuran (THF), and *N*-bromosuccinimide (NBS) were purchased from Sigma–Aldrich (Steinheim, Germany). Dichloromethane (DCM) (>98) and acetonitrile (HPLC grade), acetone (ACS, ISO) were supplied from Merck (Darmstadt, Germany). Alumina polishing suspension (0.05 CB micron Gamma Type, CR85S) was obtained from Balkowski International All chemicals were high grade reagents and used as received. Multi-walled carbon nanotubes had the following properties: average diameter: 8–15 nm, length: ≈ 30 μm, purity: > 95%, specific surface area[48] (SSA): 350 $m^2\ g^{-1}$, (Hayzen Engineering, Ankara/Turkey).

### Instrumentation

An Iviumstat model potasiostat/galvanostat (software, iviumsoft and Faraday cage, BASI Cell Stand $C_3$) was used for electrochemical studies, which was equipped with a three-electrode electrochemical cell, employing GCE (glassy carbon electrode) as a working electrode, platinum disk as a counter electrode, encapsulated in epoxy resin (*geometric area*: 0.020 $cm^2$) and a saturated calomel electrode (SCE) as a reference electrode. All potentials were presented on the SCE scale.

FTIR spectra of $Th_4DTT$ and P($Th_4DTT$) on ITO was recorded with an ATR-FTIR Nicolet 6700. Electropolymerization of $Th_4DTT$ on ITO was performed in 0.1 M $TBABF_4$/DCM solution with a constant potential of +1.5 V.

Digital microscope (TENSION), ultrasonic bath (Elma, E3OH, Elmasonic), deionized water equipment (purelab Option-Q, ELGA, DV25), accurate balance (OHAUS Pioneer), incubator (DRY-Line, VWR) were used in various experimental steps.

### EIS and Modeling

Electrochemical impedance spectroscopy (EIS) measurements were recorded at room temperature (25°C ± 1°C), using a conventional three electrode cell configuration. EIS measurements were conducted in monomer-free electrolyte solutions with a perturbation amplitude 10 mV with a frequency range of 10 mHz to 100 kHz on an Iviumstat Model Potasiostat/Galvanostat (software; iviumsoft). The circuit model parameters were obtained by Zsimpwin 3.22 programme.

The 3,5-bis(4-bromophenyl)dithieno[3,2-*b*;2',3'-*d*]thiophene (**2**)[49,50] and 4,4,5,5-tetramethyl-2-(thiophen-2-yl)-[1,3,2]-dioxaborolane (**4**)[51] were synthesized following the literature procedures.

#### *2,6-dibromo-3,5-bis(4-bromophenyl)dithieno[3,2-***b***; 2',3'-d]thiophene (3)*

To a solution of **2** (0.3 g, 0.59 mmol) dissolved in DMF (40 mL) was added NBS (0.316 g, 1.77 mmol) portion wise at 0°C. After stirring for 4 h, it was allowed to warm to room temperature. Then, the reaction mixture was poured into cold water

and the precipitate was filtered. The crude product was recrystallized from toluene to obtain the title compound **3** as a yellow powder (0.35 g, 88%), mp 309–312°C; $^1$H NMR (600 MHz, $CDCl_3$) $\delta$ (ppm) 7.62 (d, $J = 8.4$ Hz, 4H), 7.53 (d, $J = 8.4$ Hz, 4H); $^{13}$C NMR (150 MHz, $CDCl_3$) $\delta$ (ppm) 139.7, 136.1, 132.5, 132.1, 131.0, 128.7, 124.0, 113.6; $m/z = 667$ ($M^+ + 1$).

***2,6-di(thiophene-2-yl)-3,5-bis(4-(thiophene-2-yl) phenyl)dithieno[3,2-b;2',3'-d]thiophene (1)***

A mixture of **3** (0.3 g, 0.45 mmol), **4** (0.57 g, 2.71 mmol) and $Pd(PPh_3)_4$ (26 mg, 0.0225 mmol) in a schlenk tube was degassed for an hour. Then, THF (100 mL, dry) and $K_2CO_3$ (2 mL, 2 M) were added and degassing was continued for one more hour, after which the mixture was stirred at 65°C for 2 days. It was then cooled to room temperature, filtered through celite and washed with THF. The solvent was evaporated under reduced pressure until a concentrated solution was obtained, which was poured into a methanol/diethyl ether solution (1/1) to obtain the title compound **1** as an orange powder (0.23 g, 75%), mp 284–287°C; $^1H$ NMR ($CDCl_3$, 600 MHz): $\delta$ (ppm) 7.65 (d, $J = 8.4$ Hz, 4H), 7.51 (d, $J = 8.4$ Hz, 4H), 7.35 (d, $J = 3.6$ Hz, 2H), 7.29 (dd, $J = 5.4$ Hz, 1.2 Hz, 2H), 7.24 (dd, $J = 5.4$ Hz, 1.2 Hz, 2H), 7.09–7.08 (m, 4H), 6.98 (t, $J = 4.2$ Hz, 2H); $^{13}C$ NMR (150 MHz, $CDCl_3$) $\delta$ (ppm) 143.8, 143.1, 136.0, 134.3, 133.3, 132.3, 131.6, 129.7, 128.3, 128.1, 127.4, 126.8, 126.3, 126.2, 125.1, 123.4; MS $m/z = 677$ (M+1).

**Polymerization Procedure with Carbon Nanotube**

Carbon nanotube (CNT) (15 mg) was dispersed in supporting electrolyte sodium dodecyl sulfate (SDS) solution (5 mL 0.1*M*) for 45 min.[52] The electrode was produced by modifying the literature[53] procedure. CNT (5μL) was applied on to a glassy carbon (GC) electrode surface and dried initially in air and then by blowing nitrogen. $Th_4$DTT was electro-synthesized by chronoamperometric method in tetraethyl ammonium tetrafloroborate ($TEATF_4$, 0.1*M*)/dichloromethane ($CH_2CI_2$) solution at a constant potential of 1.2 V at different polymerization time (100, 200, 300, and 400 s). Then, nafion solution (5 μL, 5%) was dropped on to the surface of the electrode. CNT–polymer ratio was calculated by using the following formula;

$$\text{CNT \% ratio} = M_{CNT}/M_{Polym} \times 100$$

The polymer mass was calculated by using the following formula; $Q_{dep} \times M_{Mon} / Z \times F$

where *F*: Faraday constant (96485 C), $Z = 2$ (for our polymer), $Q_{dep}$: Deposition charge, $M_{Mon}$: mass of monomer.

**Calculation of Specific Capacitance with Cyclic Voltammetry**

Cyclic voltammograms and electrochemical impedance spectroscopy data for $[Th_4DTT]_0 = 2$ m*M* and 3 m*M* in total solution of 5 mL of $H_2SO_4$ (0.5*M*) were measured and specific capacitance calculated by using two different formulas.

Specific capacitance (*Sc*)

$$Sc = \Delta Q / M \times \Delta V \quad (1)$$

where $\Delta Q$; Voltammetric charge integrated from cyclic voltammogram (*C*), $\Delta V$; Potential range (*V*),[54] *M*; Mass of the electrode material on the electrode surface (g), calculated by using the following formula;

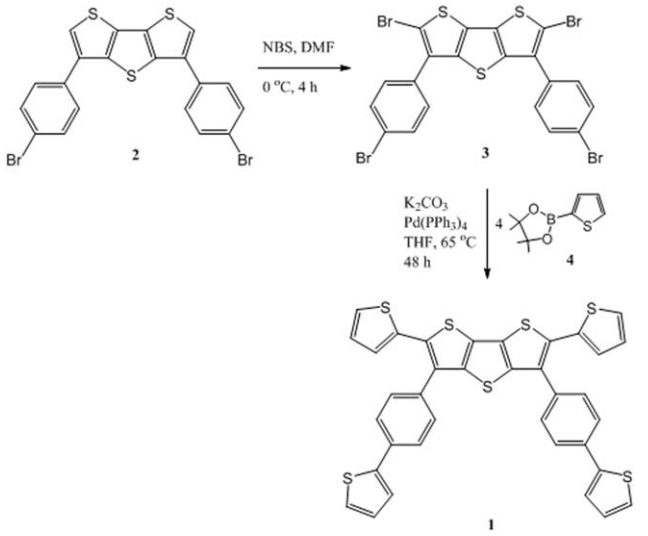


**Figure 1.** Synthesis of 2,6-di(thiophen-2-yl)-3,5-bis(4-(thiophen-2-yl)phenyl)dithieno[3,2-*b*;2',3'-*d*]thiophene, ($Th_4$DTT).

$$M = M_{CNT} + M_{Polym}$$

$$Sc = \int I \times dV / S \times m \times \Delta V \quad (2)$$

where $\int(I \times dV)$; area integrated from CV, *S*; scan rate (mV $s^{-1}$), $\Delta V$; potential range and *m*; mass of the electrode material on the electrode surface (g).[55,56]

EIS was measured in $H_2SO_4$ 0.5 (M) in monomer-free solution at different scan rates of 25, 50, 100, 250 for polymers, coated with CNT for 100, 200, 300, 400 s.

## RESULTS & DISCUSSION

**Synthesis of $Th_4$DTT 1**

The 2,6-di(thiophene-2-yl)−3,5-bis(4-(thiophene-2-yl)phenyl)-dithieno[3,2-*b*;2',3'-*d*] thiophene ($Th_4$DTT) **1** was synthesized in two steps (Figure 1). Dibromination of the DTT **2** with NBS produced the tetrabromo-DTT **3** in 88% yield,[57] Suzuki coupling of which with 4,4,5,5-tetramethyl-2-(thiophene-2-yl)[1,3,2]dioxaborolane **4** yielded the target compound **1** in 75%.

**Electrocopolymerization**

$Th_4$DTT was electropolymerized by chronoamperometric method at different polymerization time (100, 200, 300, and 400 s) in 0.1*M* $TEABF_4$/DCM at a constant potential of 1.2 V. The highest specific capacitance (20.17 F $g^{-1}$) was obtained for P($Th_4$DTT)/MWCNT in the initial monomer concentration of 2 m*M* at the polymerization time of 100 s (Figure 2).

Cyclic voltammetry (CV) measurements of the composite electrode, i.e. P($Th_4$DTT)/MWCNT, was conducted in $H_2SO_4$ (0.5*M*) solution at various scan rates of 25, 50, 100, 250, 500, and 1000 mV $s^{-1}$ (Figure 3). The specific capacitances were obtained from the area and charge formulas of CV (Table I), which indicated that the highest $C_{sp}$ was 20.17 F $g^{-1}$ for P($Th_4$DTT)/MWCNT in the scan rate of 100 mV $s^{-1}$. It means that $C_{sp}$ was increased ~10 times in area and charge formulas compared to P($Th_4$DTT). Generally, combination of

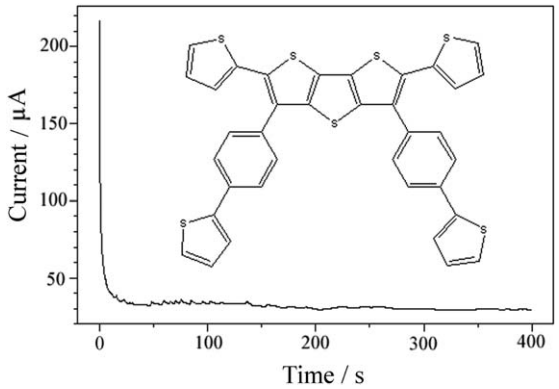


**Figure 2.** $Th_4DTT$/MWCNT was electrocoated by chronoamperometric method in 0.1 M $TEABF_4$/DCM at a constant potential of 1.2 V in 400 s. $[Th_4DTT]_0$= 2 m*M*.

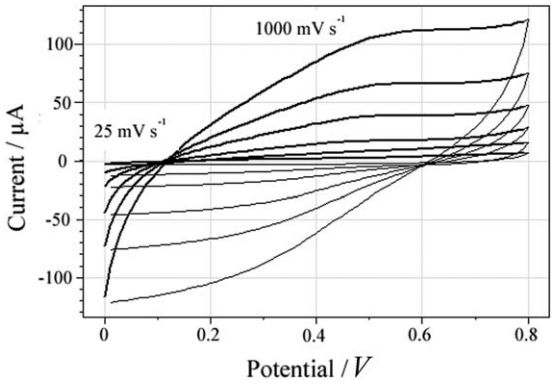


**Figure 3.** Cyclic voltammograms of $Th_4DTT$/MWCNT electrodes in $H_2SO_4$ solution (0.5*M*) at a scan rate of 25, 50, 100, 250, 500, and 1000 mV $s^{-1}$.

P($Th_4DTT$)/MWCNT is based on electrochemical interaction onto the surface of CNTs by covalent bonding.[58–61]

Specific capacitance (Sc) obtained from area and charge formulas are nearly the same values by changing of scan rates. For example, at the scan rate of 25 mV $s^{-1}$, Sc was obtained as 1.62 F $g^{-1}$ from area formula and 1.69 F $g^{-1}$ from charge formula. The similar results were obtained for composite (P($Th_4DTT$)/CNT) materials such as Sc = 15.39 F $g^{-1}$ from area formula and Sc= 15.35 F $g^{-1}$ from charge formula as shown in Table I.

### FTIR Analysis of Monomer and Polymer

The FTIR-ATR spectra of $Th_4DTT$ in 0.1*M* $TEABF_4$/DCM was obtained by reflectance FTIR spectrophotometry (Figure 4). The peak at 940 $cm^{-1}$ was attributed to dopant anion $BF_4^-$. While the peak at 2950 $cm^{-1}$ was due to symmetric stretch of C═C—H of benzene ring, the peak at 720 $cm^{-1}$ was assigned to C—S stretch of thiophene ring. Typical broad polymeric bands belonging to the polymer, P($Th_4DTT$), compare with more sharper bands of the monomer $Th_4DTT$, proved a successful polymerization process.

### SEM-EDX Analyses of the Polymer and the Composite

Morphological studies of P($Th_4DTT$) and P($Th_4DTT$)/MWCNT samples were performed by scanning electron microscopy. SEM images of the polymer and composite, obtained at 30-µm magnification are depicted in Figure 5(a,b), respectively. While the SEM image of P($Th_4DTT$) displayed only a porous structure having small and bigger pores with ~5 and ~20 µm sizes, respectively [Figure 5(a)], SEM image of P(Th4DTT)/MWCNT showed homogeneously scattered strand like structure [Figure 5(b)].

EDX analyses of P($Th_4DTT$) and P($Th_4DTT$)/MWCNT indicated a clear difference between P($Th_4DTT$) and P($Th_4DTT$)/MWCNT as P($Th_4DTT$)/MWCNT had a composite material structure, in which the weight percent of carbon, fluorine and sulfur elements decreased in 21.60, 59.79, and 1.27%, respectively, as the weight percent of nitrogen and sodium elements increased in 16.64 and 0.70%, respectively. Moreover, nitrogen and sodium elements were obtained in composite structures from SDS and MWCNT. Therefore, EDX analyses indicated a successful composite structure formation (Table II).

### *Capacitor Behaviors of P($Th_4DTT$) and P($Th_4DTT$)/MWCNT Obtained from Circuit Model* $R_s(C_1(R_1(Q(R_2W))))(C_2R_3)$

The polymer and composite were evaluated by employing ZSimpWin 3.22 software from Princeton Applied Research. The circuit model $R_s(C_1(R_1(Q(R_2W))))(C_2R_3)$was obtained almost among 90 circuit models as its chi-square ($\chi^2$) and relative error were below $10^{-4}$ and 10%, respectively. In circuit components, $R_s$ is the bulk solution resistance of the polymer and electrolyte, $C_1$ and $R_1$ are the double layer capacitance and resistance of the polymer and electrolyte, respectively. A series connection to $R_1$ was established using as a constant phase element parallel to $R_2$ and *W*, which are the charge transfer resistance and Warburg

**Table I.** Specific Capacitances Obtained by Chronoamperometric Method (400 s) from Area, and Charge Formulas at Different of Scan Rates from 25 to 1000 mV $s^{-1}$ for P($Th_4DTT$) and P($Th_4DTT$)/CNT, $[Th_4DTT]_0$= 2 m*M*

| | P($Th_4DTT$) | P($Th_4DTT$)/CNT | P($Th_4DTT$) | P($Th_4DTT$)/CNT |
|---|---|---|---|---|
| Scan rates/mV $s^{-1}$ | Area/F $g^{-1}$ | Area/F $g^{-1}$ | Q/F $g^{-1}$ | Q/F $g^{-1}$ |
| 25 | 1.62 | 15.39 | 1.69 | 15.35 |
| 50 | 0.58 | 20.12 | 0.58 | 20.05 |
| 100 | 2.17 | 20.17 | 2.24 | 20.17 |
| 250 | 0.17 | 16.78 | 1.72 | 16.38 |
| 500 | 0.13 | 13.71 | 1.34 | 13.61 |
| 1000 | 0.10 | 10.84 | 0.99 | 10.84 |

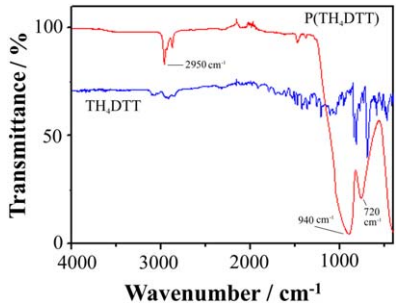


**Figure 4.** FTIR spectra of $Th_4DTT$ and P($Th_4DTT$). Electropolymerization of $Th_4DTT$ on ITO was performed in 0.1*M* $TBABF_4$/DCM solution with a constant potential of +1.5 V. [Color figure can be viewed in the online issue, which is available at wileyonlinelibrary.com.]

impedance of the polymer and composite, respectively.[62] The Warburg impedance is often observed at high frequencies, which is signaling some type of anomalous diffusion process. *Q-n* (constant phase element) defines the capacitor between the film and electrolyte interface, considering the irregular geometry of the surface of the composite electrode.[63,64] Comparison of the polymer and composite simulation results are given in Table III. $R_s$ value of polymer ($R_s = 126\ \Omega$) decreased with comparison of the composite material ($R_s = 25.74\ \Omega$). In parallel to these results, $C_{sp}$ and $C_{dl}$ values increased in Nyquist and Bode-magnitude plots, as well as equivalent circuit parameters. The circuit parameters and SEM images indicated that the polymer and composite material had inhomogeneous surface morphology.

Low frequency capacitance ($C_{sp}$) values for P($Th_4DTT$) and P($Th_4DTT$)/MWCNT (10 mHz) were obtained by using the following equation: $C_{sp} = (2\pi \times f \times Z'')^{-1}$, where $C_{sp}$ is the specific capacitance, $Z''$ is the slope of a plot of the imaginary component of impedance versus the inverse of the frequency ($f$).[65,66] While the $C_{sp}$ value of P($Th_4DTT$) was determined to be 0.31 mF $cm^{-2}$, P($Th_4DTT$)/MWCNT had the $C_{sp}$ as 4.01 mF $cm^{-2}$, which indicated that the composite material had 15 times higher $C_{sp}$ than that of the polymer (Figure 7).

Double layer capacitance ($C_{dl}$) can be calculated from a Bode-magnitude plot, by extrapolating the linear section to a value of $\omega = 1$ ($\log \omega = 0$), a formula of $|Z| = 1/C_{dl}$ (Figure 8). The $C_{dl}$ value of the composite material (4.43 mF $cm^{-2}$) was found to be ~25 times higher than that of the $C_{dl}$ value of the polymer

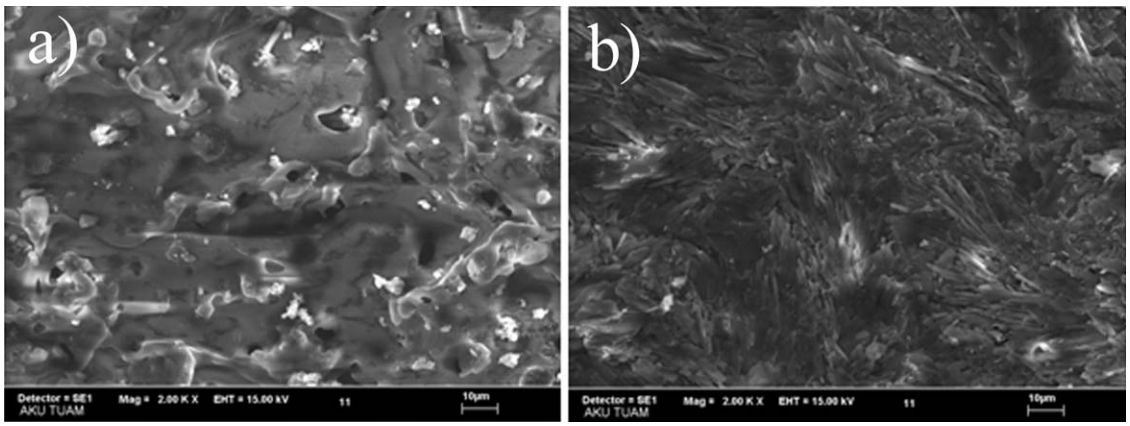


**Figure 5.** SEM images of (a) P($Th_4DTT$) and (b) P($Th_4DTT$)/MWCNT. Electropolymerization of $Th_4DTT$ on Au electrode was performed in 0.1*M* $TEABF_4$/DCM solution with a constant potential of +1.2 V in 400 s. $[Th_4DTT]_0 = 2$ m*M*.

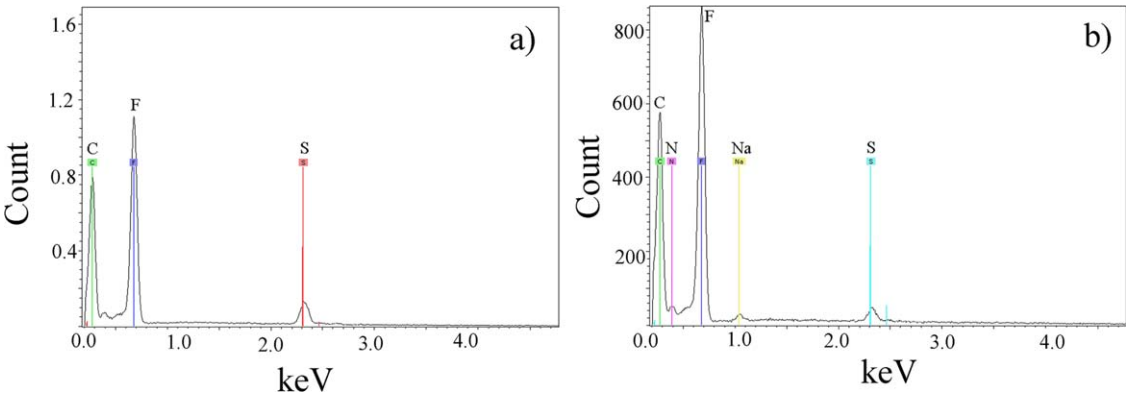


**Figure 6.** EDX images of (a) P($Th_4DTT$) and (b) P($Th_4DTT$)/MWCNT. Electropolymerization of $Th_4DTT$ on Au electrode was performed in 0.1*M* $TEABF_4$/DCM solution with a constant potential of +1.2 V in 400 s. $[Th_4DTT]_0 = 2$ m*M*. [Color figure can be viewed in the online issue, which is available at wileyonlinelibrary.com.]

**Table II.** EDX Analyses of (a) P($Th_4$DTT) and (b) P($Th_4$DTT)/CNT

| Elements/% | P($Th_4$DTT) | P($Th_4$DTT)/CNT |
|---|---|---|
| Carbon | 32.69 | 21.60 |
| Fluorine | 69.36 | 59.79 |
| Sulfur | 3.95 | 1.27 |
| Nitrogen | ..... | 16.64 |
| Sodium | ..... | 0.70 |

Electropolymerization of $Th_4$DTT on Au electrode was performed in 0.1 M $TEABF_4/CH_2Cl_2$ solution with a constant potential of +1.2 V in 400 s. $[Th_4DTT]_0$= 2 mM.

(0.18 mF $cm^{-2}$). The increasing value of $C_{dl}$ could be explained due to the incorporation of MWCNT into the polymer.

The maximum phase angles of the composite material and polymer were measured to be $\theta = 60.7°$ and $\theta = 51.6°$, respectively, at 1 Hz frequency (Figure 9). When the frequency was increased up to $10^3$, the phase angle decreased ~20° and, in the higher frequencies, the phase angle increased sharply [Figure 9(b)].[67] Charge storage of the composite electrode had an increase of charge storage at the frequency of ~1 Hz to 60.7° [Figure 9(a)] compared with the charge storage of the polymer at 51.6° [Figure 9(b)].[68] Theoretically, Bode-phase angle is nearly close to 90° as observed in a capacitor behavior.[69]

**Table III.** Equivalent Electrical Circuit Model, $R_s(C_1(R_1(Q(R_2W))))(C_2R_3)$, Parameters for P($Th_4$DTT) and P($Th_4$DTT)/CNT in 0.1*M* $TEABF_4$/$CH_2Cl_2$ Solution by Chronoamperometric Method with a Constant Potential of +1.2 V in 400 s

| Circuit components | P($Th_4$DTT) | P($Th_4$DTT) / CNT |
|---|---|---|
| $R_s/\Omega$ | 126 | 25.74 |
| $C_1/\mu F$ | $1.4 \times 10^{-2}$ | 0.91 |
| $R_1/\Omega$ | 2760 | 163.1 |
| $Q\text{-}Y_o/S\times s^n$ | $4.1 \times 10^{-6}$ | $8.6 \times 10^{-3}$ |
| $n$ | 0.61 | 0.66 |
| $R_2/\Omega$ | $9.64 \times 10^5$ | $6.64 \times 10^5$ |
| $W/\mu S\times s^{-n}$ | 1.68 | 2.02 |
| $C_2/\mu F$ | $3.0 \times 10^{-3}$ | 0.14 |
| $R_3/\Omega$ | 1577 | 10 72.4 |
| $\chi^2$ | $1.83 \times 10^{-4}$ | $5.73 \times 10^{-4}$ |

$[Th_4DTT]_0$= 2 mM.

The average conductivity of P($Th_4$DTT)/MWCNT was found to be 19.5 mS, obtained from Admittance plot by EIS analysis, at the frequency of 100 kHz (Figure 10). On the other hand, the conductivity of P($Th_4$DTT) ($Y'' = 1.29$ mS) was measured to be 15 times lower than that of the composite material (Table III).

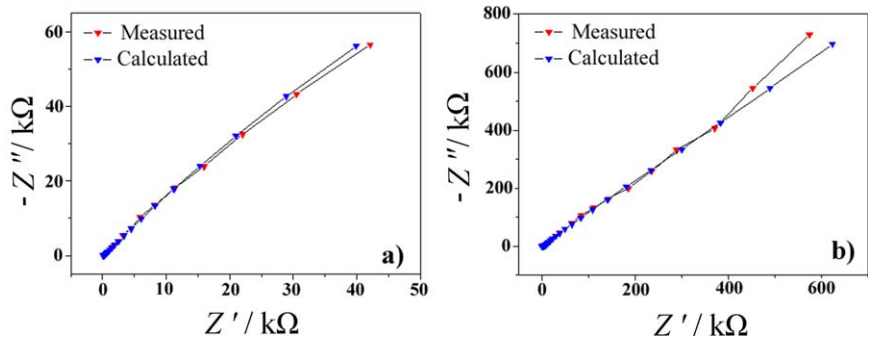


**Figure 7.** Nyquist plots of (a) P($Th_4$DTT)/MWCNT, and (b) P($Th_4$DTT), $[Th_4DTT]_0 = 2$ m*M* in $H_2SO_4$ (0.5*M*). Polymerization was performed by chronoamperometric method (400 s). [Color figure can be viewed in the online issue, which is available at wileyonlinelibrary.com.]

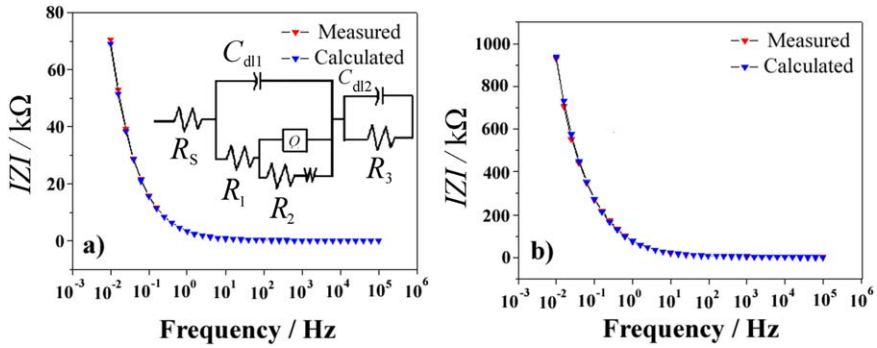


**Figure 8.** Bode-magnitude plots of (a) P($Th_4$DTT)/MWCNT, inset: Equivalent circuit model of $R_s(C_1(R_1(Q(R_2W))))(C_2R_3)$ and (b) P($Th_4$DTT), $[Th_4DTT]_0 = 2$ m*M* in $H_2SO_4$ (0.5*M*). Polymerization was performed by chronoamperometric method (400 s). [Color figure can be viewed in the online issue, which is available at wileyonlinelibrary.com.]

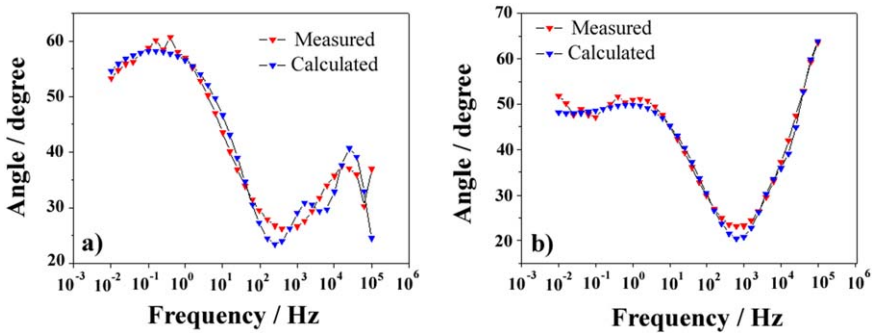


**Figure 9.** Bode-phase plots of (a) P($Th_4$DTT)/MWCNT, and (b) P($Th_4$DTT), [$Th_4$DTT]$_0$ = 2 m*M* in $H_2SO_4$ (0.5*M*). Polymerization was performed by chronoamperometric method (400 s). [Color figure can be viewed in the online issue, which is available at wileyonlinelibrary.com.]

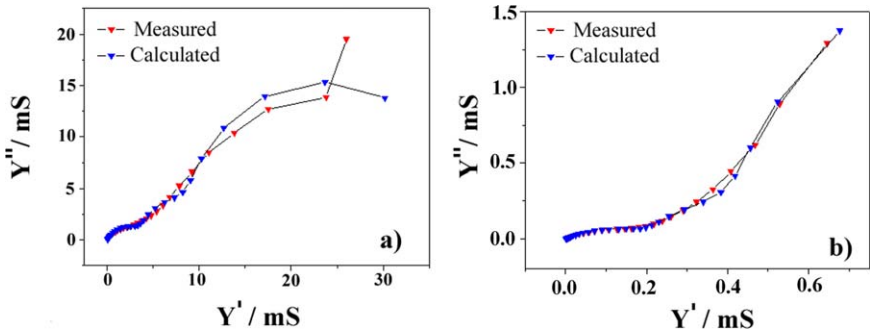


**Figure 10.** Admittance plots of (a) P($Th_4$DTT)/MWCNT, and (b) P($Th_4$DTT), [$Th_4$DTT]$_0$= 2 m*M* in $H_2SO_4$ (0.5*M*). Polymerization was performed by chronoamperometric method (400 s). [Color figure can be viewed in the online issue, which is available at wileyonlinelibrary.com.]

### Stability of Polymer Film

As it is well-known, long-term stability is a significant consideration for the practical application of a capacitor. Stability measurement for P($Th_4$DTT)/MWCNT system was performed with a scan rate of 100 mV $s^{-1}$ through the same voltage (0–0.8 V) over 500 cycles. Long-term stability of the capacitor was also tested by CV, and the result of the specific capacitance was found to still at 87.37% of the initial capacitance (Figure 11), which indicated that the composite P($Th_4$DTT)/MWCNT is suitable for the capacitor applications as it had high stability for practical applications.

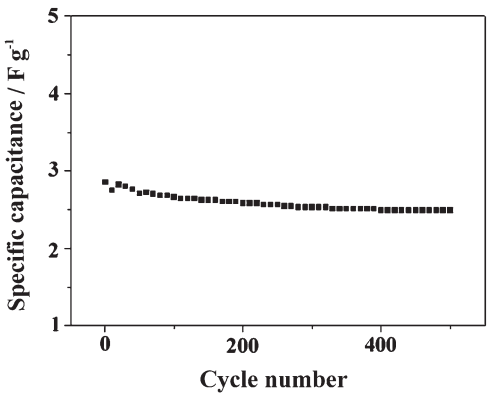


**Figure 11.** Stability test measurements of P($Th_4$DTT)/MWCNT. Potential range: 0–0.8 V, scan rate: 100 mV $s^{-1}$. Nearly 500 cycles were performed for stability test. $C_{sp}$ was calculated and plotted on the graph at every 10 cycle.

## CONCLUSION

In this study, synthesis and characterization of a novel compound, 2,6-di (thiophene-2-yl)−3,5bis(4-(thiophene-2-yl)phenyl)dithieno [3,2-*b*;2′,3′-*d*]thiophene, ($Th_4$DTT) have been reported. Its electro-deposition, applying chronoamperometric method on glassy carbon electrode as a composition with MWCNT was conducted, and comparison of the specific capacitance of P($Th_4$DTT) and P($Th_4$DTT)/MWCNT composite were studied in $H_2SO_4$ (0.5*M*) by cyclic voltammetry (CV). $C_{sp}$ obtained from the area and charge formulas was determined as 20.17 F $g^{-1}$ with a scan rate of 100 mV $s^{-1}$. An equivalent circuit model of $R_s(C_1(R_1(Q(R_2W))))(C_2R_3)$ was used to fit the theoretical and experimental data. Nyquist, Bode-magnitude, Bode-phase and Admittance plots were obtained to explain the impedance parameters. The $C_{sp}$ value of P($Th_4$DTT)/MWCNT (4.01 mF $cm^{-2}$) was found to be ~15 times higher than that of P($Th_4$DTT) (0.31 mF $cm^{-2}$), and long-term stability test by CV measurements indicated that the specific capacitance of the composite was still 87.37% of the initial capacitance.

To our best knowledge this the first report on capacitor behavior of a dithienothiophene as the composite P($Th_4$DTT)/MWCNT displayed a good capacitive characteristics.

## AUTHOR CONTRIBUTIONS

The manuscript was written through the contributions of all authors. All authors have given approval to the final version of the manuscript.

## ACKNOWLEDGMENTS

The authors thank Serhat Tikiz (Afyon Kocatepe Univ., TUAM, Afyon, Turkey) for SEM-EDX measurements, Istanbul Technical University (Istanbul, Turkey) for a grant to Suzan Baslilar (MSc) and Unsped Global Lojistik for financial support.

## REFERENCES

1. Brodd, R. J.; Bullock, K. R.; Leising, R. A.; Middaugh, R. L.; Miller, J. R.; Takeuchi, E. *J. Electrochem. Soc.* **2004**, *151*, 1.
2. Portet, C.; Taberna, P. L.; Simon, P.; Flahaut, E.; Laberty-Robert, C. *Electrochim. Acta*, **2005**, *50*, 41.
3. Kotz, R.; Carlen, M. *Electrochim. Acta*, **2000**, *45*, 2483.
4. Hu, Y.; Zhao, Y.; Li, Y.; Li, H.; Shao, H.; Qu, L. *Electrochim. Acta*, **2012**, *66*, 279.
5. Conway, B. E.; Birss, V.; Wojtowicz, J. *J. Power Sources*, **1997**, *66*, 1.
6. Girija, T. C.; Sangaranarayanan, M. V. *J. Power Sources*, **2006**, *156*, 705.
7. Kiebooms, R.; Menon, R.; Lee, K. In Handbook of Advanced Electronic and Photonic Materials and Devices; Nalwa, H. S., Ed.; Academic Press: San Diego, **2001**; Vol. *8*, 321.
8. Fonseca, C. P.; Benedetti, E. J.; Neves, S. *J. Power Sources*, **2006**, *158*, 789.
9. Cooper, A. I. *J. Mater. Chem.*, **2000**, *10*, 207.
10. Groenendaal, L.; Zotti, G.; Aubert, P. H.; Waybright, S. M.; Reynolds, J. R. *Adv. Mater.* **2003**, *15*, 855.
11. Pappenfus, T. M.; Chesterfield, R. J.; Frisbie, C. D.; Mann, K. R.; Casado, J.; Raff, J. D.; Miller, L. L. *J. Am. Chem. Soc.*, **2002**, *124*, 4184.
12. Shirota, Y. *J. Mater. Chem.*, **2000**, *10*, 1.
13. Andersson, M. R.; Thomas, O.; Mammo, W.; Svensson, M.; Theander, M.; Inganas, O. *J. Mater. Chem.*, **1999**, *9*, 1933.
14. Albert, K. J.; Lewis, N. S.; Schauer, C. L.; Sotzing, G. A.; Stitzel, S. E.; Vaid, T. P.; Walt, D. R. *Chem. Rev.*, **2000**, *100*, 2595.
15. Chrisey, D. B.; Horwitz, J. S.; Leuchtner, R. E. *Thin Solid Films*, **1991**, *206*, 111.
16. Cocchib, V.; Guadagninia, L.; Mignania, A.; Salatelli, E.; Tonelli, D. *Electrochim. Acta*, **2011**, *56*, 6976.
17. Beaupre, S.; Leclerc, M. *Adv. Funct. Mater.*, **2002**, *12*, 192.
18. Watson, K. J.; Wolfe, P. S.; Nguyen, S. T.; Zhu, J.; Mirkin, C. A. *Macromolecules*, **2000**, *33*, 4628.
19. Lai, C.; Guo, W.; Tang, X.; Zhang, G.; Pan, Q.; Pei, M. *Synth. Met.*, **2011**, *161*, 1886.
20. Iijima, S., *Nature*, **1991**, *354*, 56.
21. Byrne, M. T.; Gun'ko, Y. K. *Adv. Mater.*, **2010**, *22*, 1672.
22. Collins, P. G.; Avouris, P. *Sci. Am.*, **2000**, *283*, 62.
23. Esawi, A. M. K.; Farag, M. M. *Mater. Des.*, **2006**, *28*, 2394.
24. Ajayan, P. M.; Schadler, L. S.; Braun, P. V.; Ajayan, P. M.; Schadler, L. S.; Braun, P. V. Nanocomposite Science and Technology; Wiley VCH: New York, **2003**.
25. Nayak, S.; Bhattacharjee, S.; Bimal, P. S. *Carbon*, **2012**, *50*, 4269.
26. Baibarac, M.; Gomez-Romero, P. *Nanosci. Nanotechnol.*, **2006**, *6*, 289.
27. Hatchett, D. W.; Josowicz, M. *Chem. Rev.* **2008**, *108*, 746.
28. Srivastava, R. K.; Srivastava, A.; Prakash, R.; Singh, V. N.; Mehata, B. R. *J. Nanosci. Nanotechnol.*, **2009**, *9*, 5382.
29. Hughes, M.; Chen, G. Z.; Shaffer, M. S. P.; Fray, D. J.; Windle, A. H. *Chem. Mater.*, **2002**, *14*, 1610.
30. Wang, J.; Dai, J.; Yarlagadda, T. *Langmuir*, **2005**, *21*, 9.
31. Sainz, R.; Benito, A. M.; Martinez, M. T.; Galindo, J. F.; Sotres, J.; Baro, A. M.; Corraze, B.; Chauvet, B. O.; Maser, W. K. *Adv. Mater.*, **2005**, *17*, 278.
32. Ajayan, P. M. *Chem. Rev.*, **1999**, *99*, 1787.
33. Tasis, D.; Tagmatarchis, N.; Bianco, A.; Prato, M. *Chem. Rev.* **2006**, *106*, 1105.
34. Jeon, I. Y.; Kang, S. W.; Tan, L. S.; Baek, J. B. *J. Polym. Sci. Polym. Chem.* **2010**, *48*, 3103.
35. Kymakis, E.; Amaratunga, G. A. *J. Appl. Phys. Lett.*, **2002**, *80*, 1435.
36. Miller, A. J.; Hatton, R. A.; Silva, S. R. P. *Appl. Phys. Lett.*, **2006**, *89*, 123115.
37. Cheung, W.; Chiu, P. L.; Parajuli, R. R.; Ma, Y.; Ali, S. R.; He, H. *J. Mater. Chem.*, **2009**, *19*, 6465.
38. Yoon, H.; Ko, S.; Jang, J. *J. Phys. Chem. B*, **2008**, *112*, 9992.
39. Li, L.; Qin, Z. Y.; Liang, X.; Fan, Q. Q.; Lu, Y. Q.; Wu, W. H.; Zhu, M. F. *J. Phys. Chem. C*, **2009**, *113*, 5502.
40. Reddy, K. R.; Jeong, H. M.; Raghu, A. V. *J. Polym. Sci. Polym. Chem.* **2010**, *48*, 1477.
41. Joshi, L.; Singh, A. K.; Prakash, P. *Mater. Chem. Phys.*, **2012**, *135*, 80.
42. Woo, H. S.; Czerw, R.; Webster, S.; Carroll, D. L. *Synth. Met.*, **2001**, *116*, 369.
43. Kymakis, E.; Amaratunga, G. A. *J. Appl. Phys. Lett.*, **2002**, *80*, 1435.
44. Ago, H.; Petritsch, K.; Shaffer, M. S. P.; Windle, A. H.; Friend, R. H. *Adv. Mater.* **1999**, *11*, 1281.
45. Wu, T. M.; Lin, Y. W. *Polymer*, **2006**, *47*, 3576.
46. Frackowiak, E.; Khomenko, V.; Jurewicz, K.; Lota, K.; Beguin, F. *J. Power Sources*, **2006**, *153*, 413.
47. Zhou, Y.; Qin, Z.; Li, L.; Zhang, Y.; Wie, Y.; Wang, L.; Zhu, M. *Electrochim. Acta*, **2010**, *55*, 3904.
48. Peigney, A.; Laurent, C.; Flahaut, E.; Bacsa, R. R.; Rousset, A. *Carbon*, **2001**, *39*, 507.
49. Ertas, I.; Ozturk, E. *Tetrahedron Lett.*, **2004**, *45*, 3405.
50. Osken, I.; Bildirir, H.; Ozturk, T. *Thin Solid Films*, **2011**, *519*, 7707.

51. Lo, C.; Hsu, C. *J. Polym. Sci. A Polym. Chem.*, **2011**, *49*, 3355.
52. Zhang, X.; Zhang, J.; Liu, Z. *Carbon*, **2005**, *43*, 2186.
53. Fu, C.; Haihui, Z.; Liu, R.; Huang, Z.; Chen, J.; Kuangi, Y. *Mater. Chem. Phys.* **2012**, *132*, 596.
54. Aradilla, D.; Estrany, F.; Alemán, C. *J. Phys. Chem. C*, **2011**, *115*, 8430.
55. Davies, A.; Audette, P.; Farrow, B.; Hassan, F.; Chen, Z.; Choi, J. Y.; Yu, A. *J. Phys. Chem. C*, **2011**, *115*, 17612.
56. Lai, L.; Yang, H.; Wang, L.; The, B. K.; Zhong, J.; Chou, H.; Chen, L.; Chen, W.; Shen, Z.; Ruoff, R. S.; Lin, J. *ACS Nano*, **2012**, *6*, 5941.
57. Ozturk, T.; Ertas, E.; Mert, O. *Tetrahedron*, **2005**, *61*, 11055.
58. Xu, J.; Yao, P.; Li, X.; He, F. *Mater. Sci. Eng. B*, **2008**, *151*, 210.
59. Zhao, B.; Hu, H.; Haddon, R. C. *Adv. Funct. Mater.*, **2004**, *14*, 71.
60. Gopalan, A. I.; Lee, K. P.; Santhosh, P.; Kim, K. S.; Nho, Y. C. *Compos. Sci. Technol.* **2007**, *67*, 900.
61. Ates, M.; Karazehir, T.; Arican, F.; Eren, N. *Iranian Polym. J.* **2013**, *22*, 199.
62. Ates, M.; Uludag, N.; Sarac, A. S. *Mater. Chem. Phys.*, **2011**, *127*, 120.
63. Lang, G.; Bacskai, J.; Inzelt, G. *Electrochim. Acta*, **1993**, *38*, 773.
64. Ates, M.; Sarac, A. S. *J. Appl. Electrochem.*, **2009**, *39*, 2043.
65. Ates, M.; Uludag, N. *Fibers Polym.*, **2010**, *11*, 331.
66. Fiordiponti, P.; Pistoria, G. *Electrochim. Acta*, **1989**, *34*, 215.
67. Bisquert, J.; Garcia-Belmonte, G.; Fabregat-Santiago, F.; Bueno, P. R. *J. Electroanal. Chem.*, **1999**, *475*, 152.
68. Macdonald, J. R. *J. Electroanal. Chem.*, **1987**, *223*, 25.
69. Ates, M.; Uludag, N.; Sarac, A. S. *Fibers Polym.*, **2011**, *12*, 8.